International Journal of Minerals, Metallurgy and Materials
Volume 28, Number 9, September 2021, Page 1453
https://doi.org/10.1007/s12613-020-2103-3

Reduction of NO_x emission based on optimized proportions of mill scale and coke breeze in sintering process

Zhi-gang Que[1,2], *Xian-bin Ai*[1], *and Sheng-li Wu*[2]

1) Institute of Energy Research, Jiangxi Academy of Science, Nanchang 330096, China
2) School of Metallurgical and Ecological Engineering, University of Science and Technology Beijing, Beijing 100083, China
(Received: 4 March 2020; revised: 18 May 2020; accepted: 19 May 2020)

Abstract: Reducing NO_x emission of iron ore sintering process in a cost effective manner is a challenge for the iron and steel industry at present. Effects of the proportion of mill scale and coke breeze on the NO_x emission, strength of sinter, and sinter indexes were studied by combustion and sinter pot tests. Results showed that the peak value of NO concentration, total of NO emission, and fuel-N conversion rate gradually decreased as the proportions of the mill scale increased because NO was reduced to N_2 by Fe_3O_4, FeO, and Fe in the mill scale. The strength of sinter reached the highest value at 8.0wt% mill scale due to the formation of minerals with low melting point. The fuel-N conversion rate slightly fluctuated and total NO_x emission significantly decreased with the decreased proportions of coke breeze because CO formation and content of N element in the sintered mixture decreased. However, the sinter strength also decreased due to the decrease in the amount of the melting minerals. Furthermore, results of the sinter pot tests indicated that NO_x emission decreased. The sinter indexes performed well when the proportions of mill scale and coke breeze were 8.0wt% and 3.70wt% respectively in the sintered mixture.

Keywords: iron ore sinter; NO_x emission; mill scale; coke breeze; proportion optimization

1. Introduction

As crude steel production gradually increases in China, NO_x emissions of iron and steel industry increase annually, thereby causing environmental pollution in forms such as acidic rain and photochemical smog, which are hazardous to human health and social development. The iron and steel manufacturing industry is an important source of NO_x emission, whose NO_x emission accounts for over 6% of that from all industries in China [1–3]. Moreover, approximately 50% of the NO_x emission of the steel industry was from sintering [3–6]. Thus, reducing NO_x emissions in the sintering process is needed to ensure environmental protection.

NO_x is the fuel-NO_x type during the sintering process and is mainly generated through the combustion of solid fuels such as coke breeze and anthracite. NO represents the majority of fuel-NO_x, accounting for approximately 95wt% [7–9]. NO_x emission in the sintering process is mainly related to the formation and reduction of NO. In recent years, many studies have been conducted on inhibiting nitrogen oxidation and promoting NO reduction in the sintering process. For instance, some researchers [10–14] found that the existing state of coke breeze remarkably affects its combustion behavior during sintering; the percentage of C-type coke and combustibility of coke increased, whereas the NO emission decreased due to the transformation of S-type coke to S'-type coke. Other researchers [15–20] studied the influences of coke breeze particle size on the CO and NO concentrations during the combustion process and found the existence of an appropriate size. Studying the effects of lime-coating coke on the NO_x concentration, references [21–25] found that CaO inhibited the coke combustion at low temperature and promoted coke combustion at high temperature. Pan [15], Gan *et al*. [26–28], and Morioka *et al*. [29] observed that calcium ferrite minerals could promote the reduction of NO to N_2 by CO, resulting in reduced NO_x emission. NO_x was also reduced to N_2 by the transition metals or their oxides. Xiong *et al.* [30] found that the decomposition of NO to N_2 was promoted by TiO_2 or V_2O_5 of iron ore. Wu *et al*. [31] and Reddy and Khanna [32] also observed that NO was reduced to N_2 by Fe_3O_4, FeO, and Fe. Kasai *et al.* [33] proposed the reduction of NO_x emission by pre-mixing metallic iron or iron ore with coke breeze. Nakano *et al*. [34] found that a decrease in fuel nitrogen in the sinter mix was due to substitution of metallic

Corresponding author: Zhi-gang Que E-mail: quezhigang@126.com

iron for coke breeze, thereby reducing the NO_x emissions in the sintering process.

Although the aforementioned studies have clarified the reduction of NO to N_2 by iron oxide and NO_x emission was reduced by substituting metallic iron for coke breeze, further work is necessary because the influences of metallic-iron bearing resource on the NO_x reduction process and the sinter indexes are complex. Mill scale is an inexpensive metallic-iron bearing resource that contains Fe_2O_3, Fe_3O_4, FeO, and Fe. Thus, this study aims to reduce the NO_x emission during the sintering process by adding mill scale into the sinter mixture. The influences of the proportion of mill scale and coke breeze on the NO_x emission, sinter strength, and sinter indexes were studied through combustion and sinter pot tests. Suitable proportions of the mill scale combined with the coke breeze were proposed to reduce the NO_x emission.

2. Experimental

2.1. Raw materials

Raw sinter materials, which contained iron materials (blend ore and return fine), fluxes (quicklime, limestone, dolomite, and serpentine), and coke breeze, were obtained from a sintering plant in China. Chemical components of the raw materials are shown in Table 1. Proximate and ultimate analyses of coke breeze are listed in Table 2. Mass fractions of fixed carbon, volatile, and N element were 85.55%, 1.25%, and 0.97%, respectively. Net calorific value was 29313 kJ/kg. The mill scale formed in steelworks was dried. The chemical compositions of the mill scale are presented in Table 3. The contents of FeO and iron metal were approximately 60.00wt% and 4.57wt%, respectively. The X-ray diffraction result in Fig. 1 shows that the mill scale contains iron metal (Fe) and all three oxides of iron, namely, hematite (Fe_2O_3), magnetite (Fe_3O_4), and wustite (FeO).

Table 1. Chemical composition of raw materials wt%

Raw material	TFe	FeO	SiO_2	CaO	Al_2O_3	MgO	LOI
Blend ore	60.65	0.74	4.19	0.57	1.52	0.19	5.85
Quicklime	0.00	0.00	3.59	86.59	0.00	0.00	7.10
Limestone	0.00	0.00	0.55	54.93	0.26	0.44	43.53
Dolomite	0.00	0.00	1.43	31.13	0.34	20.23	45.60
Serpentine	0.00	0.00	38.44	2.46	0.94	37.53	13.57
Return fine	57.27	9.07	5.04	9.56	1.80	1.64	0.00
Coke breeze	0.49	0.00	5.96	0.42	3.88	0.11	87.93

Note: LOI−loss of ignition.

Table 2. Proximate and ultimate analyses of coke breeze

Proximate analysis / wt%				Ultimate analysis / wt%			Net calorific value / ($kJ \cdot kg^{-1}$)
Fixed carbon	Volatile	Ash	Moisture	C	H	N	
82.19	1.25	12.63	3.93	85.55	0.11	0.97	29313

Table 3. Chemical composition of mill scale wt%

TFe	FeO	Fe	SiO_2	CaO	Al_2O_3	MgO	S	P_2O_5	Oil
71.02	60.00	4.57	1.60	2.97	0.72	1.03	0.02	0.02	5.10

Note: TFe−Total content of Fe element.

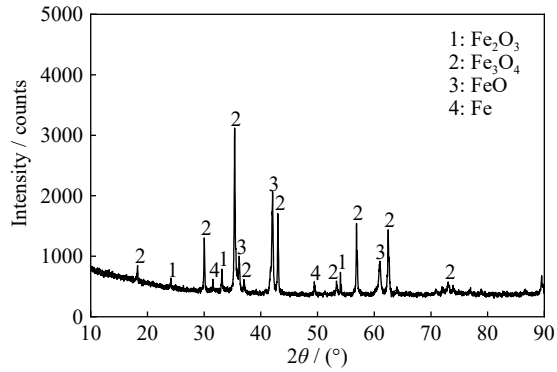

Fig. 1. XRD analysis of mill scale.

2.2. Methods

2.2.1. Combustion test

As the fuel-NO_x accounted for approximately 80wt% of the total NO_x from the sinter plant, the effect of mill scale on the coke combustion was studied. The combustion test was conducted using a horizontal furnace. A schematic of the combustion equipment is shown in Fig. 2. Samples were placed in a quartz tube with ϕ20 mm × 27 mm and then placed on a porous gasket. The coke breeze, mill scale, and alumina balls were screened to 1.8–2.0 mm. The mixture included 0.2 g coke breeze and 0.8 g mill scale or alumina balls. Before the test, the furnace was programmed to 1553 K at the heating rate of 10 K/min. The quartz tube was moved into the middle of the horizontal furnace at 7 cm/min, maintained for 5 min at object temperature, and then removed at 9.8 cm/min. The temperature of the sample is shown by thermoscouple-2 in Fig. 3. The air flow was 2 L/min during the test. The compositions of NO, CO, O_2, and CO_2 in off gas were analyzed by flue gas analyzer (MRU OPTIMA 7, Germany). As 95wt% of NO_x emission in the sintering process was NO, only NO gas was used in this study.

The evaluation indexes of fuel-N transformation were mainly the NO_x concentration, total of NO emission, and conversion rate of N element (η_N). The η_N was defined as the ratio of the mass of the N element in coke breeze oxidized to NO and the mass of the N element in coke breeze. The total

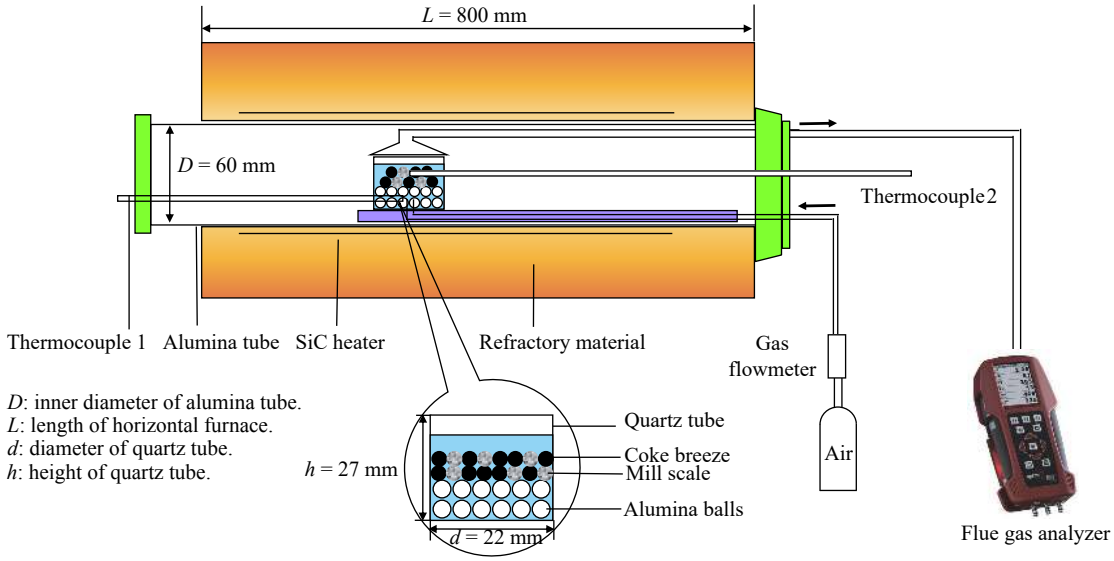

Fig. 2. Schematic of combustion equipment.

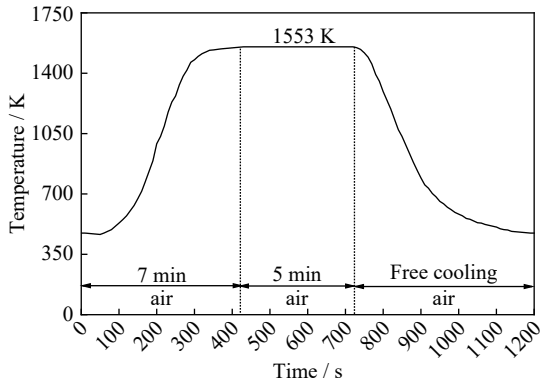

Fig. 3. Temperature and atmosphere in combustion tests.

of NO emission and conversion rate of the N element were calculated by the following equations:

$$S_{NO} = \int_0^{t_{end}} \frac{F_g C_t^{NO} M_{NO}}{60 V_{mol}} \times 10^3 dt \quad (1)$$

$$\eta_N = \frac{S_{NO} M_N}{m_{coke} \omega_{N,coke} M_{NO}} \times 100\% \quad (2)$$

where η_N (%) is the conversion rate of N element in coke breeze, S_{NO} (mg) is the mass of NO emission during the combustion test; C_t^{NO} (vol%) is the volume concentration of NO at t second; F_g (L/min) is the air flow of the combustion test; t_{end} (s) is the combustion end time; m_{coke} (mg) is the mass of coke breeze in the sample; $\omega_{N,coke}$ (wt%) is the mass fraction of N element in coke breeze; M_N (g/mol) and M_{NO} (g/mol) are the molar mass of N and NO, respectively; and V_{mol} (L/mol) is the molar volume at standard state.

2.2.2. Micro-sintering experiment

The effects of the proportions of the mill scale and coke breeze on the NO_x emission were investigated through the combustion experiment. The proportions of raw materials in the sinter mixture at different schemes are shown in Table 4. The SiO_2 and MgO contents of sinter are 4.80wt% and 1.70wt%, respectively. The basicity (CaO/SiO_2, mass ratio) of sinter was 1.80. In the A0–A3 cases, the mass ratio of the mill scale varied in the range of 0–12.0%. In the A4–A7 cases, the proportion of coke breeze was optimized when the mass ratio of the mill scale was 8.0%. In addition, the size distribution of raw materials in the sinter mixture is shown in Table 5. In the sinter mixtures, particles larger than 1.0 mm were used as cores and particles smaller than 0.5 mm were used as adhesive fines. Particles with size in the range of 0.5–1.0 mm can be used as cores and adhesive fines. Thus, to simulate the sintering process, the aforementioned particles were replaced by those with size of 1.8–2.0 mm and smaller than 0.15 mm in the micro-sintering tests. The sinter mixture, which was granulated into quasi-particles in a laboratory pelletizer, weighed 7 g in each run of the test. Then, the samples were placed in a quartz tube (ϕ20 mm × 27 mm) and sintered in a horizontal furnace. The compositions of NO, CO, O_2, and CO_2 in off gas were analyzed by gas analyzer (MRU OPTIMA 7, Germany) during the entire process and the total of NO emission and conversion rate of the N element were calculated by Eqs. (1) and (2). The temperature and atmosphere of the micro-sintering experiment were the same as that of the combustion test. After sintering, the initial mass of sinter was weighed, and then the sinter was freely dropped from 2 m high for four times. The weight of the larger than 5 mm sinter was measured. The sintering strength was defined as the ratio of the mass of a larger than 5 mm shattered sinter and the initial mass of the sinter [35–36].

2.2.3. Sinter pot test

Raw mixtures were uniformly mixed and granulated in a drum granulator. The granulated mixture was sintered in a sinter pot with 200 mm diameter and 700 mm height. The ig-

Table 4. Proportions of raw materials in sinter mixture at different schemes wt%

Raw material	A0	A1	A2	A3	A4	A5	A6	A7
Blended ore	61.72	57.90	54.07	50.23	54.18	54.31	54.47	54.69
Quicklime	3.50	3.50	3.50	3.50	3.50	3.50	3.50	3.50
Limestone	0.95	1.18	1.42	1.64	1.45	1.49	1.55	1.63
Dolomite	4.72	4.02	3.32	2.65	3.30	3.26	3.20	3.11
Serpentine	0.11	0.40	0.69	0.98	0.72	0.74	0.78	0.82
Return fine	25.00	25.00	25.00	25.00	25.00	25.00	25.00	25.00
Mill scale	0.00	4.00	8.00	12.00	8.00	8.00	8.00	8.00
Coke breeze	4.00	4.00	4.00	4.00	3.85	3.70	3.50	3.25

Table 5. Size distribution of raw materials in sinter mixture wt%

Material	>10 mm	8–10 mm	5–8 mm	3–5 mm	2–3 mm	1–2 mm	0.5–1 mm	0.25–0.5 mm	0.15–0.25 mm	<0.15 mm
Blend ore	4.28	4.41	11.24	11.99	9.96	15.67	12.41	9.83	8.10	12.75
Quicklime	0.00	0.00	0.00	0.14	1.33	4.15	6.00	12.28	14.24	61.87
Limestone	0.00	0.00	0.13	8.99	11.89	19.67	19.89	8.53	5.14	25.74
Dolomite	0.00	0.00	0.00	3.11	13.96	21.83	18.77	11.13	10.37	20.84
Serpentine	0.00	0.00	0.00	5.50	14.50	28.45	20.45	12.10	8.35	10.65
Return fine	0.49	0.97	20.54	47.61	11.83	9.10	4.79	2.25	2.43	0.00
Mill scale	3.53	1.14	8.21	3.31	6.35	21.21	25.68	13.23	9.15	8.19
Coke breeze	0.00	0.00	2.60	9.70	8.40	16.60	31.40	15.20	11.40	4.70

nition time was 120 s and suction pressure was 11.0 kPa during sintering. Moreover, the compositions of NO, CO, O_2, and CO_2 in off gas were analyzed by a flue gas analyzer (OPTIMA 7, MRU Instruments, Germany).

The sintering time was the time from the ignition to the burn-through point. The vertical sintering speed was the ratio of the initial height of the sintered bed to the sintering time (Eq. (3)). The yield was defined as the mass fraction of sinter with size over 5 mm (Eq. (4)). The productivity reflected the production efficiency of a sintering machine (Eq. (5)). According to the standard of ISO3271G75, 3 kg sinter with size between 5 and 40 mm after screening was tumbled, and then screened at 6.3 mm × 6.3 mm. After the tumbling test, $TI_{+6.3mm}$ was calculated by the mass fraction of the sinter larger than 6.3 mm (Eq. (6)). The average NO_x concentration and total NO_x emission per ton of sinter were used to evaluate the NO_x emission during the sintering process.

$$v = \frac{h}{t} \tag{3}$$

$$Y = \frac{m_0 - m_{-5.0\,\mathrm{mm}}}{m_0} \times 100\% \tag{4}$$

$$\gamma = \frac{240M}{\pi d^2 t} \times 10^3 \tag{5}$$

$$\mathrm{TI}_{+6.3\,\mathrm{mm}} = \frac{m_{+6.3\,\mathrm{mm}}}{m} \times 100\% \tag{6}$$

where v (mm/min) is the vertical sintering speed; h (mm) is the initial height of the sinter bed; t (min) is the sintering time; Y (%) is the yield of sinter; m_0 (kg) is the weight of sinter except bottom material; $m_{-5.0\,\mathrm{mm}}$ (kg) is the weight of return fines with size smaller than 5.0 mm; γ ($t \cdot m^{-2} \cdot h^{-1}$) is the productivity of sinter; M (kg) is the weight of finished sinter; d (mm) is the diameter of the sinter pot; $TI_{+6.3\,mm}$ is the tumble index of the sinter; m_0 (kg) is the mass of the sample; and $m_{+6.3\,mm}$ (kg) is the mass of the tumbled sample larger than 6.3 mm.

3. Results and discussion

3.1. Effect of mill scale on NO_x emission from coke combustion

O_2, CO_2, CO, and NO emission profiles were obtained simultaneously during coke breeze combusting. The combustion behavior of the coke breeze mixture with alumina balls or with mill scale is respectively shown in Figs. 4 (a) and 4(b). CO formed at 785 K and 792 K, and reached a peak concentration at 1121 K and 1043 K while CO_2 and NO were generated for alumina balls and mill scale, respectively. Then, CO_2 and NO reached peak concentration at 1303 K and 1363 K for alumina balls and mill scale, respectively. Compared with coke breeze mixed with alumina ball, the peak value of NO concentration (NO_{max}) decreased from 501 mg/m^3 to 283 mg/m^3 and the conversion rate of N element (η_N) decreased by 43.0% when coke breeze mixed with mill scale. Because NO was reduced to N_2 by Fe_3O_4, FeO, and Fe in the mill scale [31]. The reduction reactions between NO and iron oxides were expressed by Eqs. (7)–(10). In addition, NO was also reduced by CO during the coke breeze

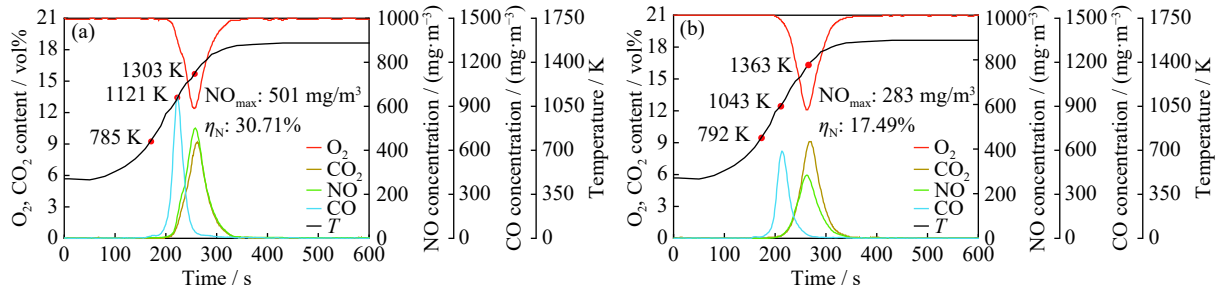

Fig. 4. O_2, CO_2, CO, and NO emission of fuel gas in coke breeze combustion tests: (a) coke breeze mixed with alumina balls; (b) coke breeze mixed with mill scale.

combustion process, and the reaction is shown in Eq. (10). The standard Gibbs free energies ($\Delta G^{\ominus}$) of Eqs. (7)–(10) were less than –160 kJ below 1573 K, which indicated that the NO could be reduced by iron oxides and CO during the sintering process.

$$4Fe_3O_4 + 2NO = 6Fe_2O_3 + N_2$$
$$\Delta G_1^{\ominus} = -660.40 + 0.3178T(\text{kJ}\cdot\text{mol}^{-1}) \quad (7)$$

$$4FeO + 2NO = 2Fe_2O_3 + N_2$$
$$\Delta G_2^{\ominus} = -747.86 + 0.2674T(\text{kJ}\cdot\text{mol}^{-1}) \quad (8)$$

$$4Fe + 6NO = 2Fe_2O_3 + 3N_2$$
$$\Delta G_3^{\ominus} = -2169.4 + 0.5820T(\text{kJ}\cdot\text{mol}^{-1}). \quad (9)$$

$$2CO + 2NO = 2CO_2 + N_2$$
$$\Delta G_4^{\ominus} = -745.71 + 0.1972T(\text{kJ}\cdot\text{mol}^{-1}). \quad (10)$$

where T is the reaction temperature, K.

3.2. Effect of proportion of mill scale on NO_x emission and sinter strength

Fig. 5 shows the NO_x emission and temperature of samples at different proportions of the mill scale in the micro-sintering experiments. Fig.5 (a) shows that the peak value of NO concentration, the total of NO emission and the conversion rate of N element decreased with the increase of the mill scale proportions. Compared with the A0 scheme, when the proportions of the mill scale were 8.0wt%, the peak value of NO concentration, the total of NO emission and the conversion rates of N decreased by 33.06%, 32.80% and 37.14%, respectively. Due to the oxidation exothermic reaction of the mill scale, the temperature of samples slightly increased between 800 and 1300 K as the proportions of the mill scale increased.

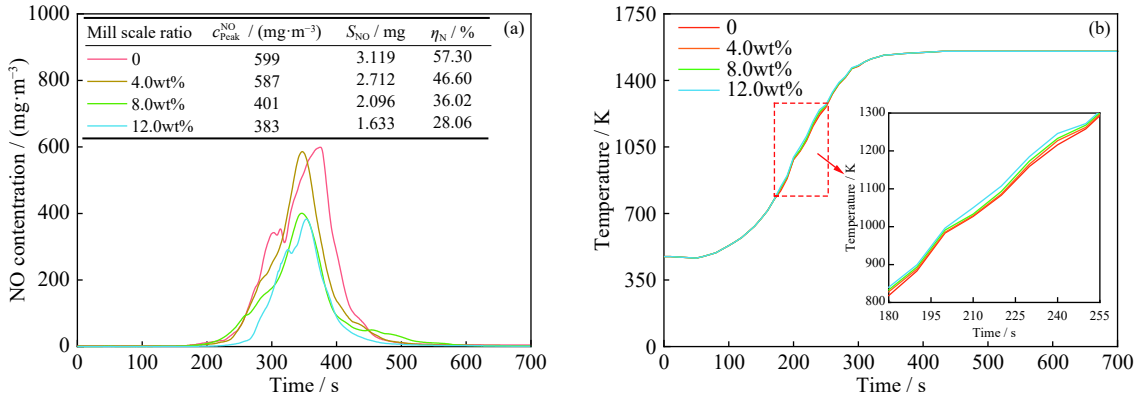

Fig. 5. NO_x emissions and the temperature of samples at different mill scale proportions: (a) NO_x emission; (b) temperature of samples.

Fig. 6 shows the strength of the sinter at different proportions of the mill scale. The figure shows that the sinter strength reached the highest point at 8.0wt% of the mill scale. Compared with the conventional condition, the sinter strength increased by 25.10% when the proportion of the mill scale was 8.0wt%. The reason may be that these participants benefited from FeO in the mill scale. On the one hand, FeO reacted with SiO_2 in the mixture to form minerals with low melting points [37–39], such as kirschsteinite. On the other hand, the sintering temperature increased due to the oxidation reaction of FeO, thereby increasing the fluidity of liquid phases. However, the low-melting-point minerals were sharply increased with the increase in the mill scale proportion from 8.0wt% to 12wt%. A thin and macroporous structure was formed, causing a decline in sinter strength.

3.3. Effect of coke breeze proportion on NO_x emission and strength of sinter with 8.0wt% mill scale

The real-time NO_x emission and temperature of samples at different proportions of coke breeze when the proportion of

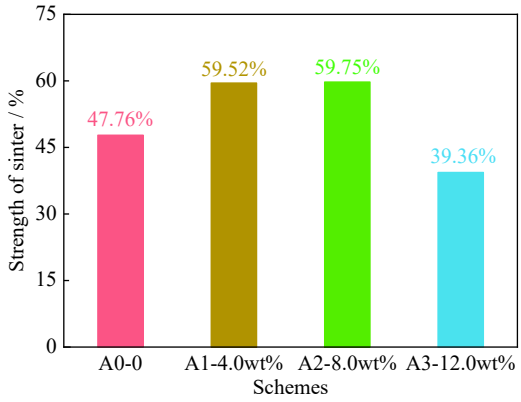

Fig. 6. Strength of sinter at different proportions of mill scale.

the mill scale was 8.0wt% is shown in Fig. 7. From Fig.7(a), we can be seen that the peak value of NO concentration firstly increased and then decreased with the proportion of coke breeze increased, reaching the highest when the proportion of coke breeze was 3.85wt%. The conversion rates of the N element slightly fluctuated, whereas the total of NO emission decreased due to the lower content of N element in raw sinter mixture. When the proportions of the coke breeze decreased from 4.00wt% to 3.70wt% and 3.25wt%, the total NO emission decreased by 5.05% and 15.3%, respectively. In addition, Fig.7(b) showed that the temperature of samples also slightly decreased between 900 and 1553 K with the proportion of coke breeze decreased. With the increasing of the proportion of coke breeze, the formation of NO_x increased, and the production of calcium ferrite minerals also increased, which promoted the reduction of NO. When the proportion of coke breeze was lower than 3.85wt%, the formations of calcium ferrite minerals were less, and the reduction efficiency of NO_x was low, resulting in NO_x emission concentration gradually increased. However, when the production of coke breeze was 4.0wt%, a large amount of calcium ferrite minerals formed, more NO_x was reduced, and then NO_x emission concentration decreased. During the sintering process, the reduction of NO by CO had a significantly influence on the conversion rate of the N element.

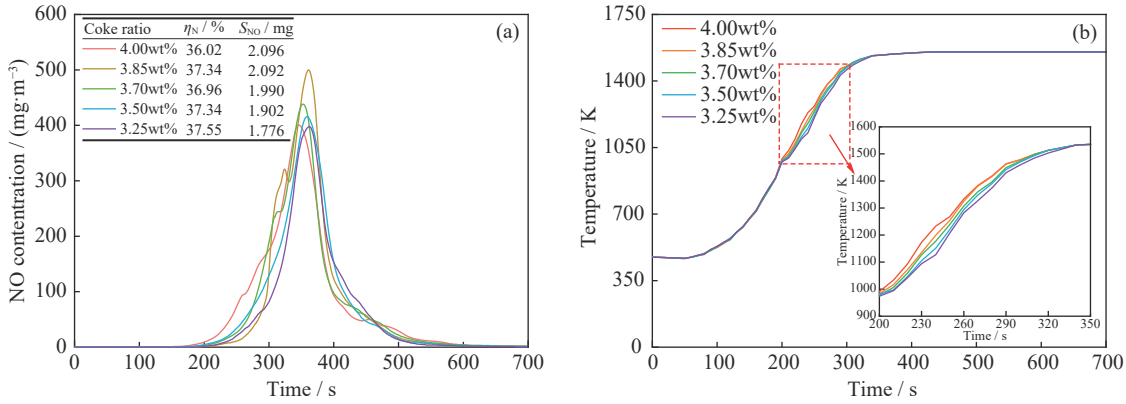

Fig. 7. NO_x emission and the temperature of samples with different proportions of coke breeze at 8.0wt% mill scale: (a) NO emission; (b) temperature of samples.

Fig. 8 shows the CO emission and correlativity of total CO emission with the conversion rate of N element in the different proportions of coke breeze. Fig. 8(a) shows that the real-time CO emission concentration exhibited an inverted V-shape trend and reached the peak value at approximately 1515 K, and then it declined to zero at the beginning of the constant temperature section (1553 K). Similar to the peak value of NO concentration, the peak value of CO concentration also firstly increased and then decreased with the proportion of coke breeze increased, reaching the maximum when the proportion of coke breeze was 3.85wt%. When the proportion of coke breeze was lower than 3.85wt%, the coke breeze was coated by the adhering fines at 1515 K, due to the strengthen of the incomplete combustion reaction, the formation of CO increased with the proportion of coke breeze increased. However, when the proportion of coke breeze increased to 4.0wt%, more heat was generated in the local areas of sintered bed, which promoted the melting of low-melting minerals, coke breeze gradually exposed and the complete combustion reaction increased, resulting in decreasing of the peak value of CO concentration. Furthermore, the total emission of CO significantly fluctuated, which was affected by the combustion behavior of coke breeze, formation of CO and the reduction behavior with NO. Fig. 8(b) shows a negative linear correlation between the total CO emission and the conversion rate of the N element. More NO was reduced as more CO formed.

The sinter strength at different proportions of coke breeze when the proportion of the mill scale was 8.0wt% is shown in Fig. 9. This figure indicates that the sinter strength gradually decreased with the decrease of the proportion of coke breeze. The sinter strength was slightly less than that of the A0 case when the proportion of coke breeze was below 3.70wt%. As the proportions of coke breeze continued to decrease, the

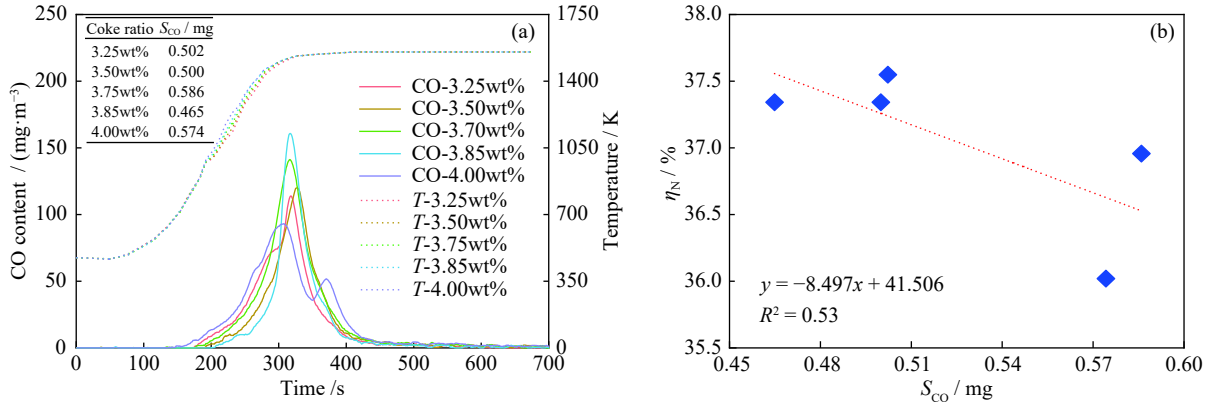

Fig. 8. CO emission and correlativity of total CO emission with conversion rate of N element in different coke breeze proportions: (a) CO emission; (b) relation of total CO emission and conversion rate of N element.

sinter strength markedly decreased by 15.87% and 38.19% in 3.50wt% and 3.25wt% of coke breeze, respectively. The highest temperature of the sintered bed decreased with a low proportion of coke breeze in the sintered mixture, thereby causing a decline in the amount of low-melting-point minerals. Thus, the proportion of coke breeze should be controlled at more than 3.70wt% to maintain the high strength of sinter.

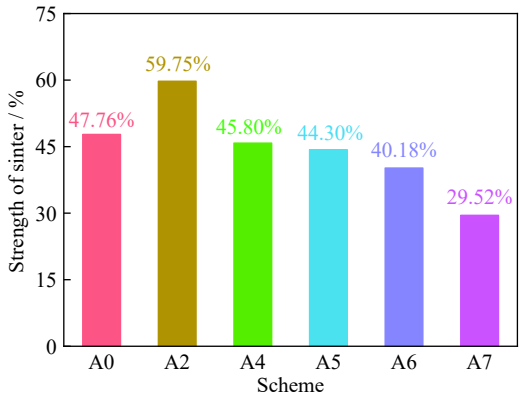

Fig. 9. Strength of sinter with different proportions of coke breeze at 8.0wt% mill scale.

3.4. Sinter pot tests

According to the preceding findings, the proportion of the mill scale and coke breeze in the sintered mixture should be controlled at 8.0wt% and more than 3.70wt%, respectively, to decrease the NO_x emission and maintain the high sinter strength. Thus, the A0, A2, A4, and A5 schemes were conducted by sinter pot test. Table 6 shows the effect of mill scale coupling with the coke breeze on the NO_x emission during the iron ore sinter process. Compared with the reference condition, in the A2 scheme, when the proportion of the mill scale was 8.0wt%, the average NO concentration and total NO_x emission per ton of sinter decreased by 9.82% and 12.90%, respectively, as NO was reduced to N_2. Meanwhile, the NO_x emission of the sintering process decreased with the decrease of the coke breeze proportions. Compared with the reference condition, when the proportion of the mill scale and coke breeze was 8.00wt% and 3.85wt% (A4 scheme), the average NO concentration and total NO_x emission per ton of sinter decreased by 19.64% and 24.19%, respectively. As the proportion of coke breeze continued to decrease to 3.70wt% (A5 scheme), the average NO concentration and total NO_x emission per ton of sinter were decreased by 39.29% and 40.32%, respectively. The content of N element decreased in the sintered mixture with the decreasing proportion of coke breeze, thereby resulting in a decline of NO formation.

Table 6. NO_x emission in sinter pot tests

Scheme	Average NO concentration / (mg·m^{-3})	Total NO_x emission per ton of sinter / (kg·t^{-1})
A0	224	0.62
A2	202	0.54
A4	180	0.47
A5	136	0.37

Table 7 shows the effects of mill scale coupling with coke breeze on the sinter indexes in the sintering process. The vertical sintering speed in the A2 scheme was significantly improved compared with the reference condition. The yield increased from 80.36% to 80.72% as the mill scale was promoted to form a greater amount of low-melting minerals. However, the productivity increased due to permeability and yield improvement deterioration. The tumble index decreased slightly since the rise of vertical sintering speed. In addition, compared with the A2 scheme, when the coke breeze was decreased, the productivity decreased because the vertical sintering speed increased and the yield decreased as less melting occurred. The tumble index was slightly decreased. Furthermore, except for the tumble index, the other sinter indexes of A5 scheme were better than those of the reference condition (A0 scheme). As a result, the proportion of coke breeze can be reduced from 4.00wt% to 3.70wt% when the proportion of the mill scale is 8.0wt% in the sintered mixture.

Table 7. Sinter indexes in sinter pot tests

Scheme	Vertical sintering speed / (mm·min^{-1})	Yield / %	Productivity / (t·m^{-2}·h^{-1})	$TI_{+6.3mm}$ / %
A0	26.81	80.36	2.00	60.00
A2	28.00	80.72	2.63	59.67
A4	33.00	80.59	2.50	58.67
A5	33.21	80.47	2.12	58.33

4. Conclusions

(1) With the proportion of the mill scale increasing from 0 to 12.0wt%, the peak value of NO concentration, the total of NO emission, and the conversion rate of N element were gradually decreased, whereas the sinter strength firstly increased and then decreased, reaching the highest value at 8.0wt% mill scale.

(2) When the proportion of the mill scale was 8.0wt%, the conversion rate of N slightly increased, but the total NO_x emission and sinter strength decreased as the proportion of coke breeze decreased. Moreover, as the proportion of coke breeze dropped below 3.70wt%, the sinter strength was significantly less than that of the reference condition.

(3) Compared with the conventional sinter condition (4.0wt% coke breeze without mill scale), 8.0wt% mill scale was added to the sintered mixture while reducing the proportion of coke breeze to 3.70wt%, the average NO concentration and total NO_x emission per ton of sinter decreased by 39.29%, 40.32%, and the tumble index decreased from 60.00% to 58.33%, other sinter indexes improved.

Acknowledgements

This work was financially supported by the National Natural Science Foundation of China (No. 51904127), the Natural Science Foundation of Jiangxi Province, China (No. 20192BAB216018), and the research and development Project (No. 2018-YYB-05) and collaborative innovation Project (No. 2018-XTPH1-05) of Jiangxi Academy of Sciences, China.

References

[1] J.M. Qie, C.X. Zhang, H.F. Wang, X.P. Li, and X.Y. Shi, Analysis of emission situation and emission reduction technology of typical sintering flue gas pollutants, *Sintering Pelletizing*, 41(2016), No. 6, p. 59.

[2] Y.D. Su, X.W. Li, and X.H. Fan, Research progress of NO_x reduction technology in sintering process, *Sintering Pelletizing*, 38(2013), No. 6, p. 41.

[3] S.L. Wu, Z.G. Que, B. Su, and Y.Z. Zhang, Research progress of the "in-bed-de NO_x" technology in iron ore sintering, *J. Eng. Stud.*, 9(2017), No. 1, p. 61.

[4] B.J. Yan, Y. Xing, P. Lu, W. Su, B. Jiang, and X.X. Cui, A critical review on the research progress of multi-pollutant collaborative control technologies of sintering flue gas in the iron and steel industry, *Chin. J. Eng.*, 40(2018), No. 7, p. 767.

[5] X.M. Yan, Y.R. Li, T.Y. Zhu, and F. Qi, Review of emission and simultaneous control of multiple pollutants from iron-steel sintering flue gas, *J. Environ. Eng. Technol.*, 5(2015), No. 2, p. 85.

[6] H.L. Zhang, Q. Shi, H.M. Long, J.X. Li, T.J. Chun, and Z.F. Gao, Analysis of NO_x removal process in sintering flue gas, *Iron Steel*, 52(2017), No. 5, p. 100.

[7] G. Suzuki, R. Ando, H. Yoshikoshi, Y. Yamaoka, and S. Nagaoka, A study of the reduction of NO_x in the waste gas from sinter plant, *Tetsu-to-Hagane*, 61(1975), No. 13, p. 2775.

[8] H. Hu, H. Huang, Z.W. Zeng, J.L. Zhang, S. Annanurov, and Q.Z. Zhao, The formation of NO_x during sintering, *Energy Sources A*, 39(2017), No. 12, p. 1228.

[9] C.B. Xu, S.L Wu, and D.Q. Cang, Numerical modeling of NO formation during packed-bed combustion of coke granules, *J. Univ. Sci. Technol. Beijing*, 7(2000), No. 4, p. 261.

[10] Y. Hida, M. Sasaki, T. Enokido, Y. Umezu, T. Iida, and S. Uno, Effect of the existing state of coke breeze in quasi-particles of raw mix on coke combustion in the sintering process, *Tetsu-to-Hagane*, 68(1982), No. 3, p. 400.

[11] E. Kasai and Y. Omori, Combustion rate of coke at different existing states prepared by fine alumina, *Tetsu-to-Hagane*, 72(1986), No. 10, p. 1537.

[12] P.L. Hou, S.M. Choi, W. Yang, E.S. Choi, and H.J. Kang, Application of intra-particle combustion model for iron ore sintering bed, *Mater. Sci. Appl.*, 2(2011), No. 5, p. 370.

[13] K.I. Ohno, K. Noda, K. Nishioka, T. Maeda, and M. Shimizu, Combustion rate of coke in quasi-particle at iron ore sintering process, *Tetsu-to-Hagane*, 101(2015), No. 3, p. 184.

[14] P.N. Ma, M. Cheng, M.X. Zhou, Y.W. Li, and H. Zhou, Combustion characteristics of different types of quasi-particles in iron ore sintering process, *Chin. J. Eng.*, 41(2019), No. 3, p. 316.

[15] J. Pan, *Theoretical and Process Studies of the Abatement of Flue Gasemissions during Iron Ore Sintering* [Dissertation], Central South University of Technology, Changsha, 2007.

[16] Z.G. Que, J.S. Wang, X.B. Ai, and S.L. Wu, Reduction of NO_x emission in sintering process based on optimization of solid fuels particle size, *China Metall.*, 29(2019), No. 6, p. 8.

[17] S.L. Wu, Y.Z. Zhang, B. Su, X.M. Wang, and L. Zhang, Analysis of main factors affecting NO_x emissions in sintering process, *Chin. J. Eng.*, 39(2017), No. 5, p. 693.

[18] Z.G. Que, S.L. Wu, G.L. Zhang, B. Su, and Y.Z. Zhang, Effect of mill scale adding methods on NO_x emission of coke combustion during iron ore sintering, [in] *AISTech and ICSTI 2015*, Cleveland, 2015, p. 1406.

[19] E. Kasai, S.L. Wu, T. Sugiyama, S. Inaba, and Y. Omori, Combustion rate and NO emission during combustion of coke granules in packed beds, *Tetsu-to-Hagane*, 78(1992), No. 7, p. 1005.

[20] Z.G. Que, S.L. Wu, and X.B. Ai, To reduce NO_x emission based on optimizing the existing states of coarse coke breeze during iron ore sintering process, *Chin. J. Eng.*, 42(2020), No. 2, p. 163.

[21] M.S. Lee and S.C. Shim, Influence of lime/limestone addition on the SO_2 and NO formation during the combustion of coke pellet, *ISIJ Int.*, 44(2004), No. 3, p. 470.

[22] K. Katayama and S. Kasama, Influence of lime coating coke on NO_x concentration in sintering process, *ISIJ Int.*, 56(2016), No. 9, p. 1563.

[23] M.Y. Gan, Z.N. Wei, C.G. Shi, H. Liu, M.F. Zhu, and T.J.

Chun, Influences of fuel modified using burnt lime on NO_x emission in burning and sintering process, *J. Iron Steel Res.*, 31(2019), No. 9, p. 816.

[24] Y.G. Chen, Z.C. Guo, Z. Wang, and G.S. Feng, NO_x reduction in the sintering process, *Int. J. Miner. Metall. Mater.*, 16(2009), No. 2, p. 143.

[25] Y.G. Chen, Z.C. Guo, and G.S. Feng, NO_x reduction by coupling combustion with recycling flue gas in iron ore sintering process, *Int. J. Miner. Metall. Mater.*, 18(2011), No. 4, p. 390.

[26] M. Gan, X.H. Fan, W. Lv, X.L. Chen, Z.Y. Ji, T. Jiang, Z.Y. Yu, and Y. Zhou, Fuel pre-granulation for reducing NO_x emissions from the iron ore sintering process, *Powder Technol.*, 301(2016), p. 478.

[27] W. Lv, X.H. Fan, X.B. Min, M. Gan, X.L. Chen, and Z.Y. Ji, Formation of nitrogen mono oxide (NO) during iron ore sintering process, *ISIJ Int.*, 58(2018), No. 2, p. 236.

[28] Z.Y. Yu, X.H. Fan, M. Gan, and X.L. Chen, Effect of Ca–Fe oxides additives on NO_x reduction in iron ore sintering, *J. Iron Steel Res. Int.*, 24(2017), No. 12, p. 1184.

[29] K. Morioka, S. Inaba, M. Shimizu, K. Ano, and T. Sugiyama, Primary application of the "in-bed-deNO_x" process using Ca–Fe oxides in iron ore sintering machines, *ISIJ Int.*, 40(2000), No. 3, p. 280.

[30] W. Xiong, J.Y. Liao, X.G. Bi, and G.F. Zhou, Experiment study of the de-NO_x in sintering waste gas, *Sintering Pelletizing*, 32(2007), No. 1, p. 12.

[31] S.L. Wu, T. Sugiyama, K. Morioka, E. Kasai, and Y. Omori, Elimination reaction of NO gas generated from coke combustion in iron ore sinter bed, *Tetsu-to-Hagane*, 80(1994), No. 4, p. 276.

[32] B.V. Reddy and S.N. Khanna, Self-stimulated NO reduction and CO oxidation by iron oxide clusters, *Phys. Rev. Lett.*, 93(2004), No. 6, art. No. 068301.

[33] E. Kasai, T. Sugiyama, and Y. Omori, Reduction of the amount of nitrogen oxides formed during sintering by using coke prepared from the mixture of coal and iron ore, *Tetsu-to-Hagane*, 80(1994), No. 4, p. 282.

[34] M. Nakano, T. Yamakawa, N. Hayakawa, and M. Nagabuchi, Effects of metallic iron bearing resources on iron ore sintering, *ISIJ Int.*, 38(1998), No. 1, p. 16.

[35] S.L. Wu, G.L. Zhang, S.G. Chen, and B. Su, Influencing factors and effects of assimilation characteristic of iron ores in sintering process, *ISIJ Int.*, 54(2014), No. 3, p. 582.

[36] G.L. Zhang, S.L. Wu, B. Su, Z.G. Que, C.G. Hou, and Y. Jiang, Influencing factor of sinter body strength and its effects on iron ore sintering indexes, *Int. J. Miner. Metall. Mater.*, 22(2015), No. 6, p. 553.

[37] C.C. Yang, D.Q. Zhu, J. Pan, and Y. Shi, Some basic properties of granules from ore blends consisting of ultrafine magnetite and hematite ores, *Int. J. Miner. Metall. Mater.*, 26(2019), No. 8, p. 953.

[38] F. Zhang, D.Q. Zhu, J. Pan, Y.P. Mo, and Z.Q. Guo, Improving the sintering performance of blends containing Canadian specularite concentrate by modifying the binding medium, *Int. J. Miner. Metall. Mater.*, 25(2018), No. 6, p. 598.

[39] S.L. Wu, B. Su, Y.H. Qi, Y. Li, and B.B. Du, Major melt formation characteristic factor analysis of iron ore liquid phase fluidity during the sintering process, *Chin. J. Eng.*, 40(2018), No. 3, p. 321.